Theory of Chiral Lipid Tubules

Jonathan V. Selinger and Joel M. Schnur
Center for Bio/Molecular Science and Engineering, Naval Research Laboratory, Code 6900, 455 Overlook Avenue, SW, Washington, D.C. 20375-5348
(Received 29 March 1993)

We present a continuum theory for the self-assembly of cylindrical tubules from chiral lipid bilayers in any tilted fluid phase. This theory shows that tubule formation is driven by an intrinsic bending force due to molecular chirality, and gives the radius in terms of the continuum parameters. The radius diverges as an untilted phase is approached. The theory also predicts that the tilt direction is modulated in a helical striped pattern on the tubule. This striped pattern is consistent with helical patterns observed in electron micrographs of lipid tubules.

PACS numbers: 87.10.+e, 61.30.−v, 68.15.+e, 87.22.Bt

The use of self-assembly to rationally control the fabrication of microstructures offers the potential for significantly improved materials. In the past decade, experiments have shown that lipid molecules self-assemble into microstructures with a variety of morphologies. Cylindrical microstructures [1–5], known as tubules, are particularly interesting for both basic research and potential applications [6,7]. Tubules are composed of bilayers or multilayers of chiral diacetylenic phosphocholine molecules, wrapped in a cylinder with a typical diameter of 0.5 μm and typical length of 50–200 μm. They exhibit a characteristic helical "barber-pole" pattern on the cylinder, as shown in Fig. 1 [8]. Similar microstructures are formed by bilayers of other chiral surfactants [9,10]. In this paper, we present a continuum theory for tubule formation driven by an intrinsic bending force in a tilted chiral bilayer [11,12]. The theory predicts the tubule radius and tilt direction, and predicts a helical pattern of stripes separated by sharp domain walls. The helical stripes are an equilibrium pattern, not an artifact of the tubule formation process. This theory explains the helical patterns observed in electron micrographs of tubules, and indicates how the structure of tubules can be controlled by varying temperature and chirality.

There have been three general approaches to the theory of tubule formation. First, de Gennes has argued that a narrow strip of a tilted chiral bilayer will buckle to form a cylinder because of its spontaneous electric polarization [13]. de Gennes's original theory considers buckling along the long axis of a cylinder, but a straightforward modification of his theory describes helical winding due to electrostatic attraction. Second, Lubensky and Prost have derived a general phase diagram for nonchiral vesicles, which predicts cylinders as well as other morphologies [14]. In the cylindrical phase, the cylinder radius and length are determined by a competition between edge energy and curvature energy. Third, Helfrich and Prost have argued that a tilted chiral bilayer will form a cylinder because of an intrinsic bending force due to chirality [11]. This theory has been extended by Ou-Yang and Liu, who model tubules by analogy with cholesteric liquid crystals [12], and by Nelson and Powers, who calculate the effects of thermal fluctuations [15]. The chiral bending force in these theories could arise from chiral molecules or from chiral symmetry breaking in the bilayer [16].

Three types of experimental results distinguish among these theories. First, experiments have shown that adding electrolytes to the solvent does not affect the formation or radius of the resulting tubules [17], except for the particular case of charged head groups [18]. This result is inconsistent with the electrostatic theories of tubule formation, because the electrostatic attraction would be screened by electrolytes in solution. Second, experiments have found no correlation between the tubule radius r and length L [2,3]. This result contradicts the modified de Gennes theory, which predicts $r \propto L^{1/3}$, and the Lubensky-Prost theory, which predicts $r \propto L^{1/2}$, and supports the other theories, which predict a fixed r independent of L. Third, the observation of helical patterns in electron micrographs of tubules implies that the tubule structure is itself chiral. This result is inconsistent with the original

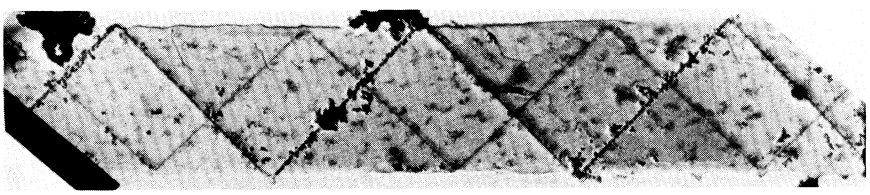

FIG. 1. Transmission electron micrograph of a tubule with adsorbed Pd/Ni catalyst particles on the surface [8]. The helical "barber-pole" pattern winding around the cylinder is consistent with the orientational domain walls predicted in this paper. In this interpretation, the domain walls appear dark because the catalyst particles preferentially adsorb there.

0031-9007/93/71(24)/4091(4)$06.00

de Gennes theory and with the Lubensky-Prost theory, which do not involve any chiral structure. Thus, only the theory of an intrinsic bending force in a tilted chiral bilayer is consistent with all of these experiments.

In this paper, we investigate how molecular chirality can induce both the formation of a cylinder and the formation of a helical pattern on the cylinder. The theory of an intrinsic chiral bending force is generalized in several ways. In our model, we assume the molecules form a bilayer in any tilted fluid phase, which may have hexatic bond-orientational order but does not have crystalline positional order. This assumption is supported by x-ray scattering results from hydrated tubules [19], and by theoretical calculations showing that a membrane that can buckle in three dimensions (3D) cannot have equilibrium crystalline order [20]. We assume the bilayer forms a cylinder of radius r and length L, as shown in Fig. 2. This structure is described by the standard cylindrical coordinates (ρ,θ,z). At any point on the cylinder, the molecular director $\hat{\mathbf{n}}$ is tilted by an angle γ with respect to the local normal $\hat{\mathbf{e}}_\rho$. The projection of $\hat{\mathbf{n}}$ into the local tangent plane makes an angle ϕ with respect to $\hat{\mathbf{e}}_\theta$. We assume that γ is uniform but ϕ may vary as a function of position, as is typically the case in flat liquid-crystal films. This contrasts with Refs. [11] and [12], which assumed that both γ and ϕ are uniform. We will investigate systematic modulations in ϕ in the mean-field ground state, and will not consider thermal fluctuations, which were studied in Ref. [15].

The free energy of a tubule is the sum of three contributions. First, there is the curvature free energy

$$F_{\text{curv}}=\int d^2x[\tfrac{1}{2}\kappa(1/r)^2], \tag{1}$$

which favors a flat bilayer. In this expression, κ is the bending rigidity. Second, there is the tilt free energy

$$F_{\text{tilt}}=\int d^2x[-\tfrac{1}{2}a\gamma^2+\tfrac{1}{4}b\gamma^4], \tag{2}$$

which favors a particular angle $\gamma=(b/a)^{1/2}$ of the director with respect to the local normal. Just below the transition to an untilted phase, a can be written as $a=\alpha(T_c-T)$, while b is approximately constant. Third, there is the Frank free energy

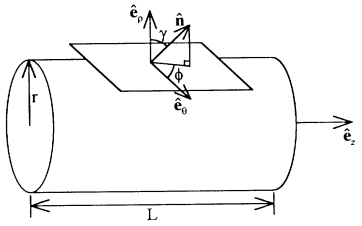

FIG. 2. The cylindrical geometry discussed in the text. The tubule has a radius r and length L. At any point on the surface, the molecular director is tilted by an angle γ with respect to the local normal vector $\hat{\mathbf{e}}_\rho$. The projection of the director into the local tangent plane is oriented at an angle ϕ with respect to $\hat{\mathbf{e}}_\theta$, the unit vector along the equator of the cylinder.

$$F_{\text{Frank}}=\int d^2x[\tfrac{1}{2}K_1|\nabla\cdot\hat{\mathbf{n}}|^2+\tfrac{1}{2}K_2|\hat{\mathbf{n}}\cdot\nabla\times\hat{\mathbf{n}}-q|^2+\tfrac{1}{2}K_3|\hat{\mathbf{n}}\times\nabla\times\hat{\mathbf{n}}|^2], \tag{3}$$

which gives the free energy for elastic distortions in $\hat{\mathbf{n}}$. Here, K_1, K_2, and K_3 are the elastic constants for splay, twist, and bend distortions, respectively. A factor of the bilayer thickness has implicitly been absorbed into these constants. For simplicity, we will make the approximation $K_1=K_2=K_3\equiv K$. The parameter q represents the chirality of the molecules. On a molecular basis, q can be interpreted as the favored angle between the orientations of neighboring chiral molecules, divided by the distance between their centers of mass. On a continuum basis, q gives the favored twist in the director field. In a nonchiral system or a racemic mixture, inversion symmetry requires $q=0$.

The total free energy $F=F_{\text{curv}}+F_{\text{tilt}}+F_{\text{Frank}}$ can be written explicitly in cylindrical coordinates as

$$F=\int d^2x\left\{\frac{\kappa}{2r^2}-\frac{a\gamma^2}{2}+\frac{b\gamma^4}{4}+\frac{K}{2r^2}\cos^2\gamma+\frac{K}{2r^2}\sin^2\gamma\cos^2\phi-\frac{Kq}{r}\sin^2\gamma\sin\phi\cos\phi+\frac{K}{r}\sin\gamma\cos\gamma\left[\frac{\partial}{r\partial\theta}(\cos\phi)+\frac{\partial}{\partial z}(\sin\phi)\right]-Kq\sin\gamma\cos\gamma\left[\frac{\partial}{r\partial\theta}(\sin\phi)-\frac{\partial}{\partial z}(\cos\phi)\right]+\frac{K}{2}\sin^2\gamma\left[\left(\frac{\partial\phi}{r\partial\theta}\right)^2+\left(\frac{\partial\phi}{\partial z}\right)^2\right]\right\}. \tag{4}$$

Note that the first six terms do not involve derivatives of ϕ, the next two terms are linear in derivatives of ϕ, and the final term is quadratic in derivatives of ϕ.

We first consider the terms that do not involve derivatives of ϕ. Minimizing these terms over ϕ gives

$$\tan 2\phi_0=-2qr, \tag{5}$$

with $45^\circ\le\phi_0\le 90^\circ$. In the limit of low curvature, $qr\gg 1$, we obtain $\phi_0=45^\circ$; i.e., the average tilt is oriented 45° from the equator of the cylinder. This is the limit studied in Refs. [11] and [12]. In the limit of extreme curvature, $qr\ll 1$, we obtain $\phi_0=90^\circ$; i.e., the average tilt is oriented along the long axis of the cylinder. Next, minimization over γ gives

$$a\gamma+\frac{K}{2r^2}(1+4q^2r^2)^{1/2}\sin 2\gamma=b\gamma^3. \tag{6}$$

This equation implicitly determines γ. Note that cylindrical curvature increases γ compared with a flat bilayer. This trend is physically reasonable because an increase in γ makes the molecules more parallel to the long axis of the cylinder, and thereby reduces the splay elastic energy. Finally, minimization over r gives

$$r=\frac{1}{q}\{\tfrac{1}{2}(A^2-1)^{1/2}[A+(A^2-1)^{1/2}]\}^{1/2}, \quad (7)$$

where

$$A=\frac{2\kappa+K+K\cos^2\gamma}{K\sin^2\gamma}. \quad (8)$$

In these equations, the chirality parameter $1/q$ sets the scale of r, and this scale is multiplied by a dimensionless factor involving γ. In the limit of small tilt, r diverges as $1/\gamma^2$. Just below the transition to an untilted phase, mean-field theory gives $\gamma\propto(T_c-T)^{1/2}$, and hence $r\propto(T_c-T)^{-1}$. Although the exact exponent will be modified by thermal fluctuations, we predict that the radius will diverge at the transition.

We now consider the terms in the free energy (4) that are linear in derivatives of ϕ. For small variations in ϕ, these terms can be written as

$$F_{\text{linear}}\approx-\int d^2x\,\lambda\hat{\mathbf{g}}\cdot\nabla\phi. \quad (9)$$

Here, the coefficient is $\lambda=K\sin\gamma\cos\gamma(r^{-2}+q^2)^{1/2}$, and $\hat{\mathbf{g}}$ is a unit vector in the local tangent plane,

$$\hat{\mathbf{g}}=\cos(\phi_0-\delta)\hat{\mathbf{e}}_\theta+\sin(\phi_0-\delta)\hat{\mathbf{e}}_z, \quad (10)$$

where $\tan\delta=1/qr$. Note that F_{linear} favors a variation of ϕ in the $\hat{\mathbf{g}}$ direction. Indeed, F_{linear} is similar to the free energy of a chiral smectic film, which was studied theoretically in Refs. [21] and [22]. As in those theories, F_{linear} can lead to a striped pattern on a tubule, with stripes perpendicular to $\hat{\mathbf{g}}$. Within each stripe, there is a gradual variation of ϕ, which makes F_{linear} negative. At the edge of each stripe, there is a sharp domain wall, where ϕ rapidly jumps back to its initial value so that the pattern can repeat periodically. The nature of the domain wall depends on the detailed structure of the bilayer phase. In the simplest case of a fluid bilayer without hexatic order, the domain wall is a narrow region where γ differs from its bulk value [22]. The wall energy per length is then approximately $E_{\text{wall}}\approx(a^2/b)(K/a)^{1/2}$. The striped pattern will occur if $\lambda>E_{\text{wall}}$. The length scale of the modulation is then limited by the terms in Eq. (4) that are quadratic in derivatives of ϕ. The resulting stripe width is approximately $(K\sin^2\gamma)/(\lambda-E_{\text{wall}})$. If the bilayer has hexatic order, then the domain-wall structure and energy change, but this argument still applies. (This argument does not apply to crystalline bilayers, but crystalline order seems to be ruled out by the experimental and theoretical arguments noted earlier.)

In Fig. 3, we illustrate the striped pattern in two limiting cases. Figure 3(a) shows the limit of low curvature, $qr\gg1$. The average tilt direction is 45° from the equator of the cylinder, and the stripes are perpendicular to the average tilt direction. In 2D, the director modulation across the stripes appears to be bend, but in 3D it is actually a combination of bend and twist, and indeed is driven by the favored twist due to molecular chirality. Figure 3(b) shows the limit of extreme curvature, $qr\ll1$. In this limit, the average tilt direction is along the long axis of the cylinder, and the stripes are parallel to the average tilt direction. The director modulation across the stripes is splay, which is driven by the curvature of the cylinder rather than by the chirality of the molecules. In 3D, the splay of the molecular director is concentrated into the domain walls rather than distributed uniformly over the cylinder. Any real system will be between these two limits.

As a comparison between these theoretical results and experiments, note that the striped pattern predicted here is consistent with the helical barber-pole pattern observed in electron micrographs of lipid tubules. As an example, Fig. 1 shows a tubule that was formed in ethanol and then placed into a dilute solution of Pd/Ni colloidal particles [8]. The helical pattern of dark lines in this micrograph corresponds to the orientational domain walls predicted by our theory. In this interpretation, the domain walls contrast with the rest of the tubules because the colloidal particles preferentially adsorb at the domain walls. Analogous accumulation of impurities at orientational domain walls has been observed directly in Langmuir monolayers [23]. Similar helical patterns are observed in cylindrical microstructures of other chiral surfactants [9,10]. In most electron micrographs, as in Fig. 1, the domain walls are oriented approximately 45° from the equator of the cylinder, which implies that the experimental tubules are close to the limit of low curvature. This result suggests that κ is large or γ is small.

Our theory could be tested further in two ways. First, one could minotor the helical pattern in a sample of tubules to see whether it anneals away in time. We predict that the pattern will be stable, because it is an equilibrium pattern rather than an artifact of the tubule formation process. Second, one could look for a periodic modulation of the tilt direction between the helical domain walls. This modulation might be observed using fluorescence microscopy with polarized laser excitation, as in Ref. [23].

Many experiments observe wound ribbons as well as closed cylinders, or even wound ribbons attached to

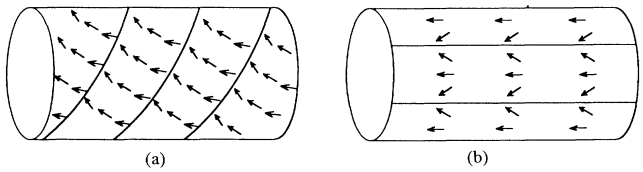

FIG. 3. Schematic views of the striped patterns in the tilt direction in two limiting cases: (a) The limit of low curvature, $qr\gg1$. (b) The limit of extreme curvature, $qr\ll1$.

closed cylinders [3]. In our theory, the orientational domain walls are natural weak lines where the cylinder can easily break, thereby forming a wound ribbon. Conversely, they are also the lines where a wound ribbon can fuse to form a cylinder. We thus expect a wound ribbon to resemble a single stripe of the pattern discussed here. In particular, we predict a modulation in the tilt direction across the width of a wound ribbon. The competition between a closed cylinder and a wound ribbon depends on the relative free energies of a domain wall in a closed cylinder and an edge of a wound ribbon.

In conclusion, we have developed a theory for cylindrical tubules of chiral lipid bilayers. We derive the radius and the average tilt direction in terms of the chirality parameter q, and in terms of the temperature near the transition to an untilted phase. Furthermore, we predict an equilibrium striped pattern on the cylinders, with stripes in the tilt direction separated by sharp domain walls. In future work, this theory could be extended in several ways. First, one could investigate modulations in the magnitude of the tilt and in the curvature of a tubule. A recent theory of rippled phases of lipid bilayers [24] suggests that the tilt modulation discussed here will necessarily lead to ripples in the curvature. Second, one could go beyond mean-field theory to investigate the effects of thermal fluctuations, using either the renormalization group or Monte Carlo simulations. Third, one could examine other morphologies of chiral lipid bilayers, such as wound ribbons, spherical vesicles, and tori. This study would give a morphology phase diagram for chiral bilayers analogous to the phase diagram of Ref. [14] for nonchiral bilayers. Finally, one could use molecular modeling to estimate q from the packing of chiral lipid molecules. Thus, models of chiral packing could relate the tubule diameter to the molecular structure. This work would extend the understanding of the general connection between chirality and pattern formation in organic microstructures.

We thank T. Gulik-Krzywicki of the Centre de Génétique Moléculaire du CNRS, Gif-sur-Yvette, France, for permission to use Fig. 1. We thank T. C. Lubensky, P. Nelson, and J. Prost for helpful discussions about this theory, and S. Baral, S. L. Brandow, J. M. Calvert, R. R. Price, B. R. Ratna, A. S. Rudolph, P. E. Schoen, R. Sashidhar, A. Singh, and D. C. Turner for helpful discussions about their experiments. This research was supported by the Office of Naval Research and the National Research Council through fellowships to J.V.S.

[1] P. Yager and P. Schoen, Mol. Cryst. Liq. Cryst. **106**, 371 (1984).

[2] J. M. Schnur, Science (to be published).

[3] J. H. Georger *et al.*, J. Am. Chem. Soc. **109**, 6169 (1987).

[4] A. S. Rudolph *et al.*, J. Am. Chem. Soc. **111**, 8516 (1989); M. Caffrey, K. Hogan, and A. S. Rudolph, Biochem. **30**, 2134 (1991); **30**, 2146 (1991); A. S. Rudolph, B. R. Ratna, and B. Khan, Nature (London) **352**, 52 (1991); M. Pazirandeh, S. Baral, and J. R. Campbell, Biomimetics **1**, 41 (1992); A. Singh and J. M. Schnur, in *Phospholipid Handbook*, edited by G. Cevc (Marcel Dekker, New York, 1993), p. 233.

[5] J. B. Lando and J. E. Hansen, Thin Solid Films **180**, 141 (1989); J. B. Lando and R. V. Sudiwala, Chem. Mater. **2**, 594 (1990).

[6] J. M. Schnur *et al.*, Polym. Preprints **28**, 440 (1987); A. S. Rudolph *et al.*, in *Biotechnological Applications of Lipid Microstructures, Advances in Experimental Medicine and Biology*, edited by B. P. Gaber *et al.* (Plenum, New York, 1989), Vol. 238, p. 305. F. Behroozi *et al.*, J. Appl. Phys. **68**, 3688 (1990); J. J. Krebs *et al.*, J. Appl. Phys. **70**, 6404 (1991); R. R. Price and M. Patchan, J. Microencapsulation **8**, 301 (1991); D. A. Kirkpatrick *et al.*, Appl. Phys. Lett. **60**, 1556 (1992).

[7] J. M. Schnur *et al.*, U.S. Patent No. 4,877,501 (1989); J. M. Schnur *et al.*, U.S. Patent No. 4,911,981 (1990); P. E. Schoen *et al.*, U.S. Patent No. 4,990,291 (1991).

[8] T. Gulik-Krzywicki and J. M. Schnur (unpublished). For related work, see P. E. Schoen *et al.*, Chem. Phys. Lipids (to be published).

[9] T. Kunitake *et al.*, J. Am. Chem. Soc. **102**, 6642 (1980); T. Kunitake, N. Nakashima, and K. Morimitsu, Chem. Lett. **1980**, 1347; N. Nakashima, H. Fukushima, and T. Kunitake, Chem. Lett. **1981**, 1207; K. Yamada *et al.*, Chem. Lett. **1984**, 1713; N. Nakashima, S. Asakuma, and T. Kunitake, J. Am. Chem. Soc. **107**, 509 (1985); T. Kunitake and N. Yamada, J. Chem. Soc. Chem. Commun. **1986**, 655.

[10] J.-H. Fuhrhop *et al.*, J. Am. Chem. Soc. **110**, 2861 (1988).

[11] W. Helfrich and J. Prost, Phys. Rev. A **38**, 3065 (1988).

[12] Ou-Yang Zhong-can and Liu Ji-xing, Phys. Rev. Lett. **65**, 1679 (1990); Phys. Rev. A **43**, 6826 (1991).

[13] P.-G. de Gennes, C. R. Acad. Sci. Paris **304**, 259 (1987).

[14] T. C. Lubensky and J. Prost, J. Phys. II (France) **2**, 371 (1992).

[15] P. Nelson and T. Powers, Phys. Rev. Lett. **69**, 3409 (1992).

[16] J. V. Selinger *et al.*, Phys. Rev. Lett. **70**, 1139 (1993).

[17] J. S. Chappell and P. Yager, Biophys. J. **60**, 952 (1991).

[18] M. A. Markowitz, J. M. Schnur, and A. Singh, Chem. Phys. Lipids **62**, 193 (1992).

[19] B. Thomas *et al.*, in *Complex Fluids*, edited by E. B. Sirota *et al.* (Materials Research Society, Pittsburgh, 1992), p. 83. Although hydrated tubules do not exhibit crystalline order, dessicated tubules are apparently crystalline (see also Ref. [5]), perhaps because dessicated tubules cannot reach equilibrium by buckling.

[20] D. R. Nelson and L. Peliti, J. Phys. (Paris) **48**, 1085 (1987); H. S. Seung and D. R. Nelson, Phys. Rev. A **38**, 1005 (1988).

[21] S. A. Langer and J. P. Sethna, Phys. Rev. A **34**, 5035 (1986).

[22] G. A. Hinshaw, R. G. Petschek, and R. A. Pelcovits, Phys. Rev. Lett. **60**, 1864 (1988); G. A. Hinshaw and R. G. Petschek, Phys. Rev. A **39**, 5914 (1989).

[23] X. Qiu *et al.*, Phys. Rev. Lett. **67**, 703 (1991).

[24] T. C. Lubensky and F. C. MacKintosh, Phys. Rev. Lett. **71**, 1565 (1993).

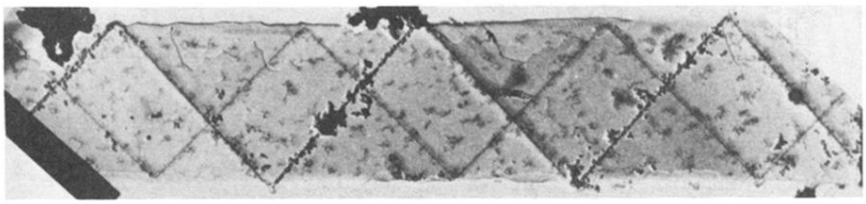

FIG. 1. Transmission electron micrograph of a tubule with adsorbed Pd/Ni catalyst particles on the surface [8]. The helical "barber-pole" pattern winding around the cylinder is consistent with the orientational domain walls predicted in this paper. In this interpretation, the domain walls appear dark because the catalyst particles preferentially adsorb there.